Continental Shelf Research ▮ (▮▮▮▮) ▮▮▮–▮▮▮

Contents lists available at SciVerse ScienceDirect

Continental Shelf Research

journal homepage: www.elsevier.com/locate/csr

Research papers

Observations and predictions of summertime winds on the Skagit tidal flats, Washington

Britt Raubenheimer [a,*], David K. Ralston [a], Steve Elgar [a], Dana Giffen [a,b], Richard P. Signell [c]

[a] Applied Ocean Physics and Engineering, Woods Hole Oceanographic Institution, Woods Hole, MA 02543, USA
[b] Anchor QEA, 720 Olive Way Seattle, WA, USA
[c] U.S. Geological Survey, Woods Hole, MA, USA

ARTICLE INFO

Article history:
Received 12 March 2011
Received in revised form
1 February 2012
Accepted 3 February 2012

Keywords:
Tidal flats
Winds
Mesoscale atmospheric model
Puget Sound

ABSTRACT

Wind speeds and directions measured in June, July, and August, 2009 at 5 locations separated by up to about 5 km on the Skagit tidal flats (near La Conner, WA) are compared with predictions of a triple-nested Weather Research and Forecast (WRF) model with 1.3-km resolution. The model predicts the observed diurnal fluctuations of the wind speeds (bias < 0.4 m s^{-1}, root-mean-square error (rmse) < 1 m s^{-1}, correlation coefficient $r^2 \approx 0.9$) and directions (bias $< 9^\circ$, rmse $< 30^\circ$, $r^2 > 0.5$). The observed and predicted minimum and maximum wind speeds occur in early morning and late afternoon, respectively. Wind speeds and directions are decorrelated over distances shorter than the length scale of the tidal flats (about 10 km). Observed and predicted wind directions are predominantly W and NW on the north flats, and S and SW on the south flats. The spatial and seasonal variability of the winds are investigated using model simulations.

1. Introduction

Owing to the shallow water depths on tidal flats, the effects of winds (and the resulting waves) on the hydrodynamics and sediment transport can be strong, even in areas with short fetches (Le Hir et al., 2000; Yang et al., 2003; Carniello et al., 2005; Manning and Bass, 2006; Manning et al., 2006; Fagherazzi et al., 2007; Ralston and Stacey, 2007; Talke and Stacey, 2008). Winds can cause changes in water levels (and thus duration of submergence over a tidal cycle), can strengthen or weaken tidal-flow asymmetries, and can cause mixing and straining (Geyer et al., 2000; Valle-Levinson et al., 2003; Scully et al., 2005; Burchard 2009; Ralston et al., this issue). For example, during low river discharge, water typically stratified during ebb tide can become completely mixed during moderate winds (less than 6 m s^{-1}). Surface plumes, and the shear just below the water surface, are strongly influenced by local winds (Henderson and Mullarney, submitted for publication). Simulations suggest that strong winds can reverse the direction of the alongshore currents (Yang et al., 2010; Nowacki and Ogston, submitted for publication). Additionally, winds generate waves, which can enhance bottom stresses, cause additional mixing, and drive mean flows (Christie et al., 1999; Christiansen et al., 2006; Mariotti and Fagherazzi, this issue). Thus, measurements or simulations of local winds are needed to model circulation, waves, and sediment transport on tidal flats (Friedrichs and Aubrey, 1996; Dyer et al., 2000; Boldt et al., submitted for publication; Ralston et al., this issue).

Winds on tidal flats surrounded by low-relief topography, such as those along the southeastern US coast, may be spatially uniform and well represented by measurements at a single nearby station. However, winds in the Puget Sound Basin (including the Skagit Bay tidal flats), which is surrounded by mountainous terrain, vary significantly over distances of only a few km. Studies of diurnal summertime winds (Mass, 1981; Ferber and Mass, 1990) have shown that northerly or westerly winds during the day arise from low pressure over the Cascade Mountains and high pressure over coastal regions, and reach a maximum in late afternoon. At night, winds weaken and come from the south or east owing to a reversal of the pressure gradient. These winds interact with the nearby mountain ranges and bodies of water to create complicated diurnal and seasonal atmospheric flow patterns (Mass, 1981; Chien and Mass, 1997). Thus, the appropriate density of observation stations or resolution of atmospheric simulations must be high to capture the spatial variability of the winds over the Skagit tidal flats.

Owing to the spatial heterogeneity of the winds in this region, it is difficult to obtain sufficient measurements to evaluate the importance of wind-driven processes. High-resolution mesoscale meteorological models have been used to provide wind forcing to drive coastal ocean circulation models (Skogseth et al., 2007; Cowles et al., 2008; Foreman et al., 2008; Liu et al., 2009).

* Corresponding author. Tel.: +1 208 255 8879.
E-mail addresses: britt@whoi.edu, braubenheimer2@whoi.edu (B. Raubenheimer).

0278-4343/$ - see front matter © 2012 Elsevier Ltd. All rights reserved.
doi:10.1016/j.csr.2012.02.001

Mesoscale models, such as the Advanced Research Weather Research and Forecasting model (WRF, Skamarock et al., 2008), have been shown to predict polar weather, large eddy turbulence, tropical cyclones, regional climate fluctuations, coastal winds, and atmospheric pollution (Snow et al., 2003; Tinis et al., 2006; Moeng et al., 2007; Davis et al., 2008). These models also predict winds well in regions with complicated, mountainous topography (Zhong and Fast, 2003; Bianco et al., 2006). In regions of complex coastal topography, highly resolved atmospheric models may be useful tools to drive surface fluxes in hydrodynamic simulations. Here, high-resolution WRF simulations are evaluated using winds observed on the Skagit tidal flats, a region that has complex topography and shallow coastal flows where local winds are important for mean currents, waves, and sediment transport.

2. Field observations

Wind speeds and directions were measured in June, July, and August 2009 at 5 locations (red symbols in Fig. 1) separated by up to about 5 km on the Skagit tidal flats in Puget Sound (near La Conner, WA).

2.1. Geographic setting

Skagit Bay is bordered by Whidbey Island to the west and by Fir Island (a deltaic area of low-lying farmland between the north and south forks of the Skagit River) to the east. Skagit Bay connects to the rest of Puget Sound through Saratoga Passage to the south and to the Strait of Juan de Fuca through Deception Pass to the north. Both of these passages are bracketed by hills up to 150 m high (Fig. 1b). West of Whidbey Island, the Strait of Juan de Fuca passes between the Olympic Mountains (with some peaks higher than 2000 m) and Vancouver Island, and connects to the Pacific Ocean (Fig. 1a). East of Skagit Bay, the Cascade Mountains also have peaks higher than 2000 m. Interactions between the low-level westerly flows from the Pacific Ocean and these mountain ranges and bodies of water create complicated atmospheric flow patterns (Mass, 1981; Chien and Mass, 1997).

2.2. Measurements

Two 3-cup anemometers mounted on towers on the north and mid flats were deployed from July 7 until August 31, 2009 at 6.1 m above the flats. These instruments were designated as N0 and N1734, respectively, where the number refers to the distance in m along the flat (parallel to Skagit Bay) from N0 (Fig. 1b). Another 3-cup anemometer was located on a tripod at the top of a small island at the east edge of the flats (July 7—August 31, 2009; 28.4 m above the flats; N1588). Two 4-bladed helicoid propeller anemometers were mounted on buoys on the south tidal flats (one deployed from June 1 to June 26 and another deployed from June 1 to July 25, 2009; both 1.2 m above the sea surface when floating; N4941 and N4193, respectively).

The spring tidal range in Skagit Bay is roughly 4 m, and at low tide, sandy tidal flats extending about 5 km west from Fir Island are exposed. Although Skagit Bay is protected from ocean swell by Whidbey Island, the local winds may drive currents and can create 1-m-high waves (Ralston et al., this issue; Webster et al., submitted for publication).

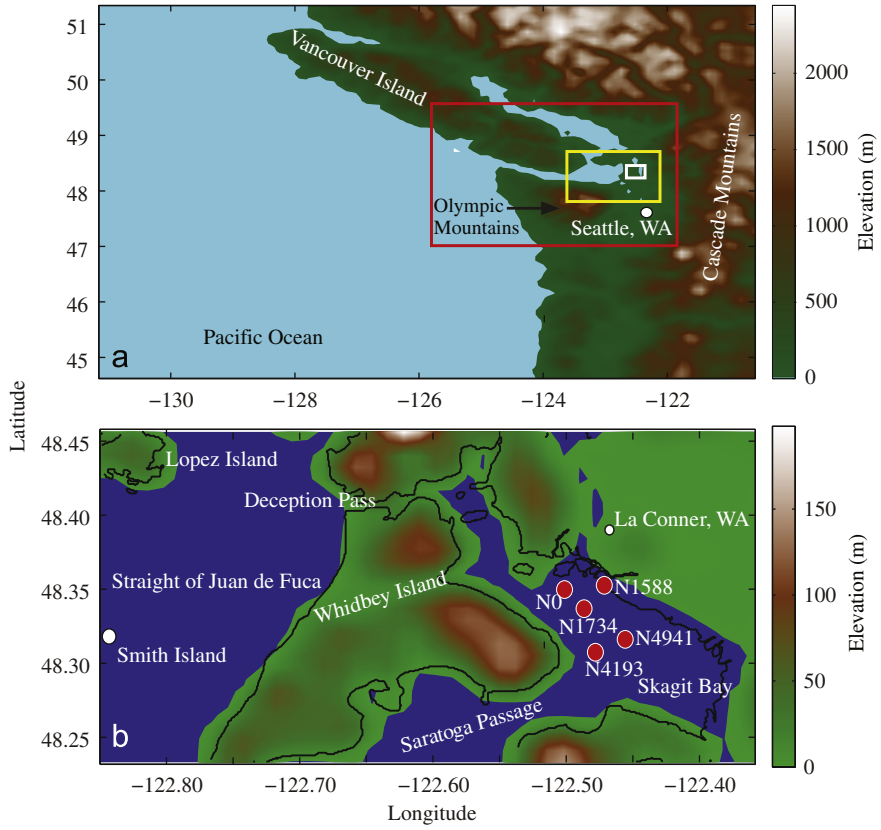

Fig. 1. (a) Region encompassed by the largest model grid (nest 1) with rectangles showing the regions for nest 2 (red), nest 3 (yellow), and the Skagit tidal flats (white), and (b) magnified image of the Skagit tidal flats region (white box in (a)) showing locations of anemometers (red circles). Colors represent topographical elevations used in (a) nest 1 (12-km resolution) and (b) nest 3 (1.3-km resolution) (scales on right). The black curve in (b) is the NOAA shoreline (http://www.ngdc.noaa.gov/mgg/coast/). Note that Puget Sound and Johnstone Pass (on the northeast side of Vancouver Island) are not well resolved by the 12-km grid, and the narrow Deception Pass is not well resolved by the 1.3-km grid.

Please cite this article as: Raubenheimer, B., et al., Observations and predictions of summertime winds on the Skagit tidal flats, Washington. Continental Shelf Research (2012), doi:10.1016/j.csr.2012.02.001

Nearbed pressure gages collocated with each anemometer were used to measure the water depth (which ranged from 0 to 4 m) and to determine times when the tidal flats were submerged or dry. At the tower and island locations, the elevation of the wind measurements above the surface was estimated by subtracting the water depth from the sensor elevation above the flats. At buoys, anemometers were estimated to be at elevations of 1.2-m above the water surface for water depths greater than 1.2 m (floating buoys), and at elevations of 2.4 m minus the water depth (buoys resting on the seafloor) for water depths less than 1.2 m.

Measured winds were converted to 10-m winds (u_{10}) assuming a logarithmic layer and neutral stability. The roughness length was estimated using Charnock's model $z_0 = \alpha u_*^2/g$ (with $\alpha = 0.015$, Charnock, 1955) when the tidal flat at the anemometer location was submerged, and using a Nikuradse rough-bed formula ($z_0 = z_s/30$, in which $z_s = 0.05$ m is the approximate height of sand ripples on the flats) when the tidal flats were exposed. The results are not sensitive to variations in α over the range $0.008 < \alpha < 0.030$ (Kraus, 1972; Smith, 1980; Sempreviva et al., 1990; Peña and Gryning, 2008). Winds were vector-averaged over hour-long periods, and rotated so that winds from true north had a direction of 0°.

Winds near the eastern end of the Strait of Juan de Fuca (measured at the National Data Buoy Center station 46088, http://www.ndbc.noaa.gov/station_page.php?station=46088) ranged from 0 to 15 m s^{-1} from the west and southwest. Winds on the tidal flats ranged from 0 to 12 m s^{-1}, usually from directions between about 150° (south-southeast) and 330° (north-northwest). Weather during the study period was unusually dry, with total precipitation of about 1 cm (< 25% of the historical average for this period) and with average air temperature about 18 °C (~2 °C warmer than average).

3. WRF model setup

Winds over the Skagit tidal flats were simulated using version 3.2 of the Advanced Research Weather Research and Forecasting model (WRF, Skamarock et al., 2008), which solves the fully compressible non-hydrostatic Euler equations of motion in flux form on a Cartesian Arakawa C grid with terrain-following sigma coordinates. The model was run using three nested grids with horizontal resolutions of 12, 4, and 1.3 km (Fig. 1). Increasing the horizontal resolution of the smallest grid to 0.8 km did not affect the results significantly. All nesting was two-way interactive, allowing continuous exchange of information between nested grids. All of the grids used 28 vertical levels with the default sigma spacing, resulting in vertical grid spacing of about 50 m near the boundary. Sensitivity of the model results to the vertical discretization was not evaluated. Default parameterizations were used (without tuning) for the model physics and dynamics, including the Monin-Obukhov scheme for surface layer physics and the heat and moisture fluxes from the surface. However, the unified Noah land surface model (Chen and Dudhia, 2001; Miao et al., 2009; Rosero et al., 2009) was used rather than the default thermal diffusion scheme to reduce instabilities. Land use and topography were input from the WRF Preprocessing System Geogrid source data package.

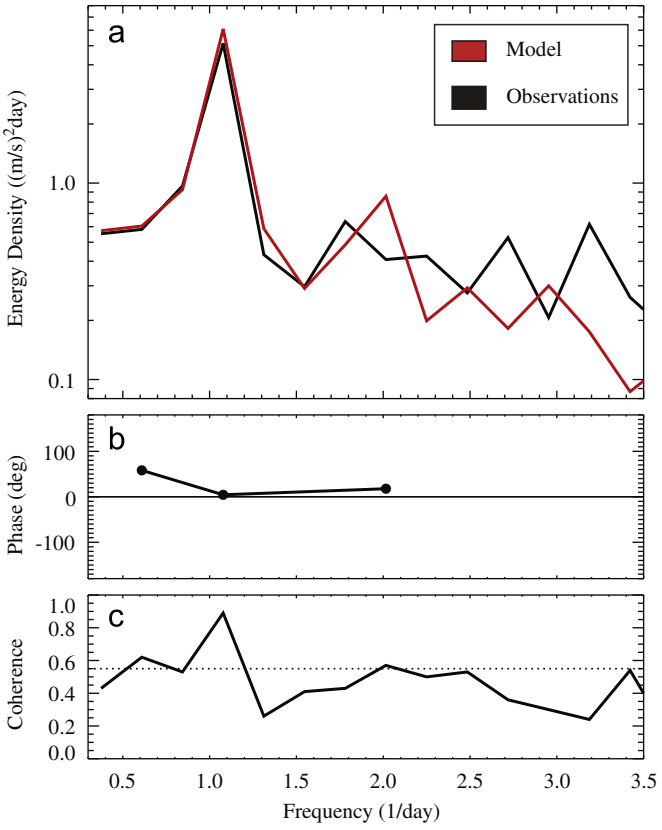

Fig. 3. (a) Observed (black curve) and predicted (red curve) wind-speed energy density at N1734 (20 degrees of freedom), (b) phase between observations and predictions (positive values suggest the observations lead the predictions), and (c) coherence between observations and predictions versus frequency. Phases are shown only when the coherence is significant (95% significance level shown by the horizontal dotted line in (c)).

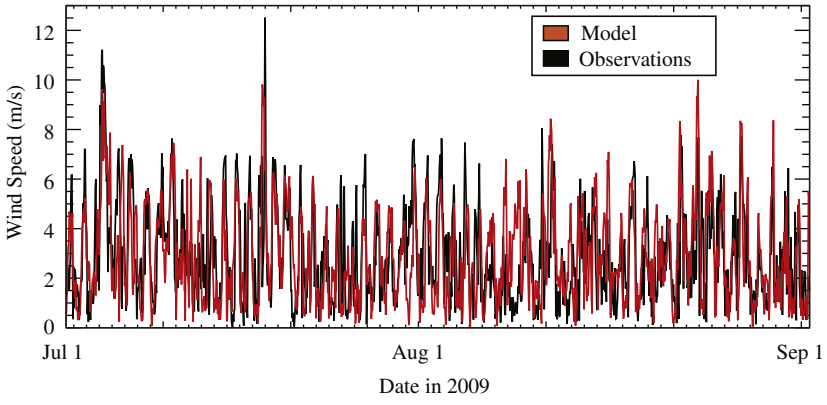

Fig. 2. Observed (black curve) and predicted (red curve) wind speed at N1734 versus time. The squared correlation between the model and data $r^2 = 0.26$, the ratio of the predicted to observed standard deviation $\sigma_{ratio} = 1.0$, the bias = 0.0 m s^{-1}, and root-mean-square model error rmse = 1.9 m s^{-1}.

Please cite this article as: Raubenheimer, B., et al., Observations and predictions of summertime winds on the Skagit tidal flats, Washington. Continental Shelf Research (2012), doi:10.1016/j.csr.2012.02.001

The nested WRF model was driven with initial and boundary conditions derived from 3- and 6-h forecast predictions of the North American Mesoscale (NAM) Model (12-km resolution), including sea-surface temperatures that were updated every 6 h. Predicted winds 10 m above the surface were output every 5 min, interpolated to the observation locations, and vector-averaged over each hour. Elevation changes over the tidal flats are small (bed slope less than 1:1000), and thus the area-averaged model cell elevations are approximately the same as point elevations and no vertical adjustments were performed. The NAM winds on the western model boundary are uncorrelated with the winds on the flats, and squared correlation coefficients of the NAM winds over the flats with the WRF model predictions at the same sites are small ($r^2 < 0.08$), indicating that the smaller-scale processes in the nested model are important to the local wind field.

4. Model-data comparisons

Observed and predicted wind speeds on the flats ranged from 0 to 12 m s^{-1} (Fig. 2). Similar to mesoscale simulations for weak to moderate synoptic forcing (Hanna and Yang, 2001; Zhong and Fast, 2003; Cheng and Steenburgh, 2005), biases (-0.2 to 0.6 m s^{-1}) and root-mean-square errors (rmse) (1.8 to 2.1 m s^{-1}) of predicted wind speeds were small for all sensor locations. However, squared correlation coefficients r^2 between observed and predicted hourly-averaged wind speeds were less than 0.3 at all sensors. Biases and rmse for wind directions were $< 10^\circ$ and $\sim 65^\circ$, respectively.

The wind-speed energy density spectrum is dominated by diurnal fluctuations, consistent with studies of summertime winds in the Puget Sound Basin (Mass, 1981; Ferber and Mass, 1990). The wind speed energy density is predicted well at diurnal frequencies (one cycle per day), with small phase lags (less than $\pm 15^\circ$) and significant coherence (0.8–0.9) at all instrument locations (e.g., Fig. 3). Coherence between the observed and predicted wind speeds usually is not significant at higher frequencies. Observed and predicted lower frequency fluctuations are significantly coherent (Fig. 3c), but the predicted winds lag the observations by up to 60° (e.g., 2.5 h at 0.6 d^{-1}, Fig. 3b).

Consistent with prior observations of diurnal summertime winds in Puget Sound Basin (Mass, 1981; Ferber and Mass, 1990), the ensemble-averaged (by hour over 24-h periods) wind speeds on the Skagit tidal flats are weakest in the morning ($\sim$7:00 PDT) and strongest in the evening ($\sim$19:00 PDT) at all instrument locations (e.g., Fig. 4a). The timing of this cycle also is similar to observed and predicted thermally- and topographically-driven winds in central Italy (Bianco et al., 2006). Ensemble-averaged wind directions on the north and mid flats are from the west-northwest in early morning, then rotate counter-clockwise ("backing"), becoming southwest or south as the wind speed reaches a minimum, and rotate clockwise back to west or west-northwest throughout the afternoon and evening (Fig. 4b). The early morning "backing" of the winds has been observed at other coastal regions, and is attributed to effects of regional topography and associated pressure systems (Orlíc et al., 1988; Zhong and Takle, 1993; Simpson, 1996; Prtenjak and Grisogono, 2007; Miao et al., 2009). Ensemble-averaged wind directions on the south flats are south to southwest, except for a short period in the afternoon when winds are west-northwest (not shown). The model predicts the ensemble-averaged diurnal wind speeds (bias < 0.4 m s^{-1}, rmse < 1 m s^{-1}, $r^2 \approx 0.9$) and directions (bias $< 9^\circ$, rmse $< 30^\circ$, $r^2 > 0.5$) reasonably well. However, similar

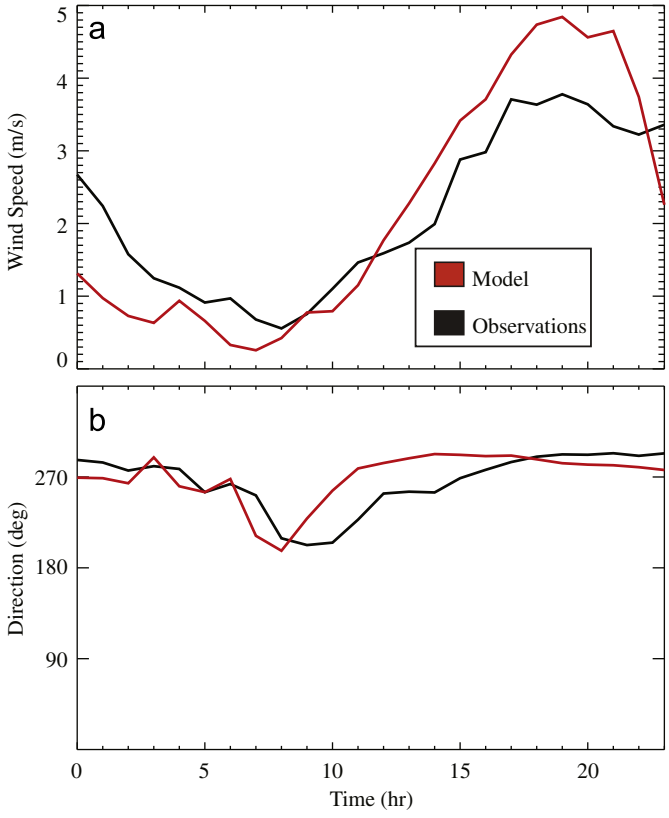

Fig. 4. Ensemble-averaged (by hour over 24-h periods) observed (black curve) and predicted (red curve) (a) wind speed and (b) direction at N1734 versus time. Hour 0 is midnight and 12 is noon PDT.

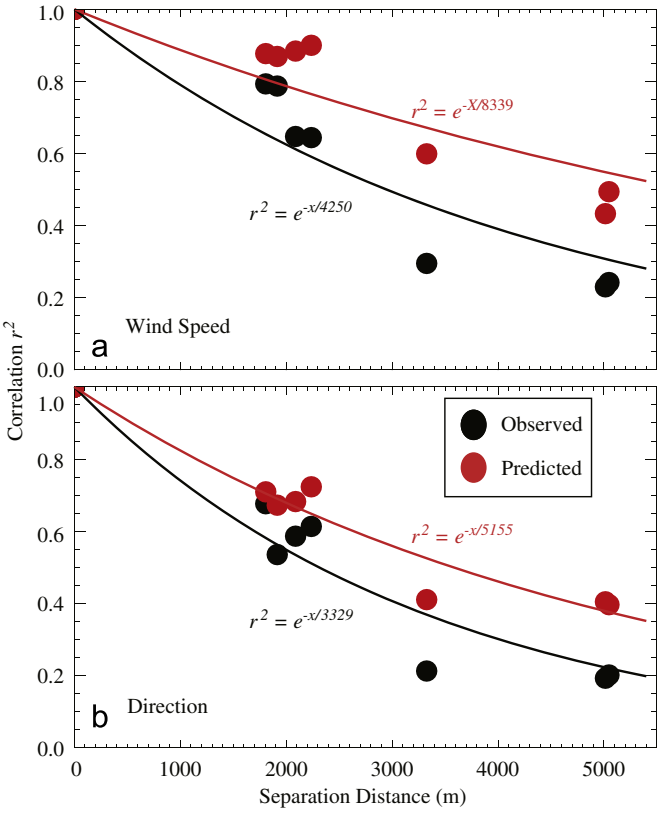

Fig. 5. Squared correlations for observed (black circles) and predicted (red circles) (a) wind speed and (b) wind direction at all pairs of anemometers on the tidal flats during July 2009 versus separation distance between each pair of locations. The best-fit exponential decays are shown by the black (observed) and red (predicted) curves.

Please cite this article as: Raubenheimer, B., et al., Observations and predictions of summertime winds on the Skagit tidal flats, Washington. Continental Shelf Research (2012), doi:10.1016/j.csr.2012.02.001

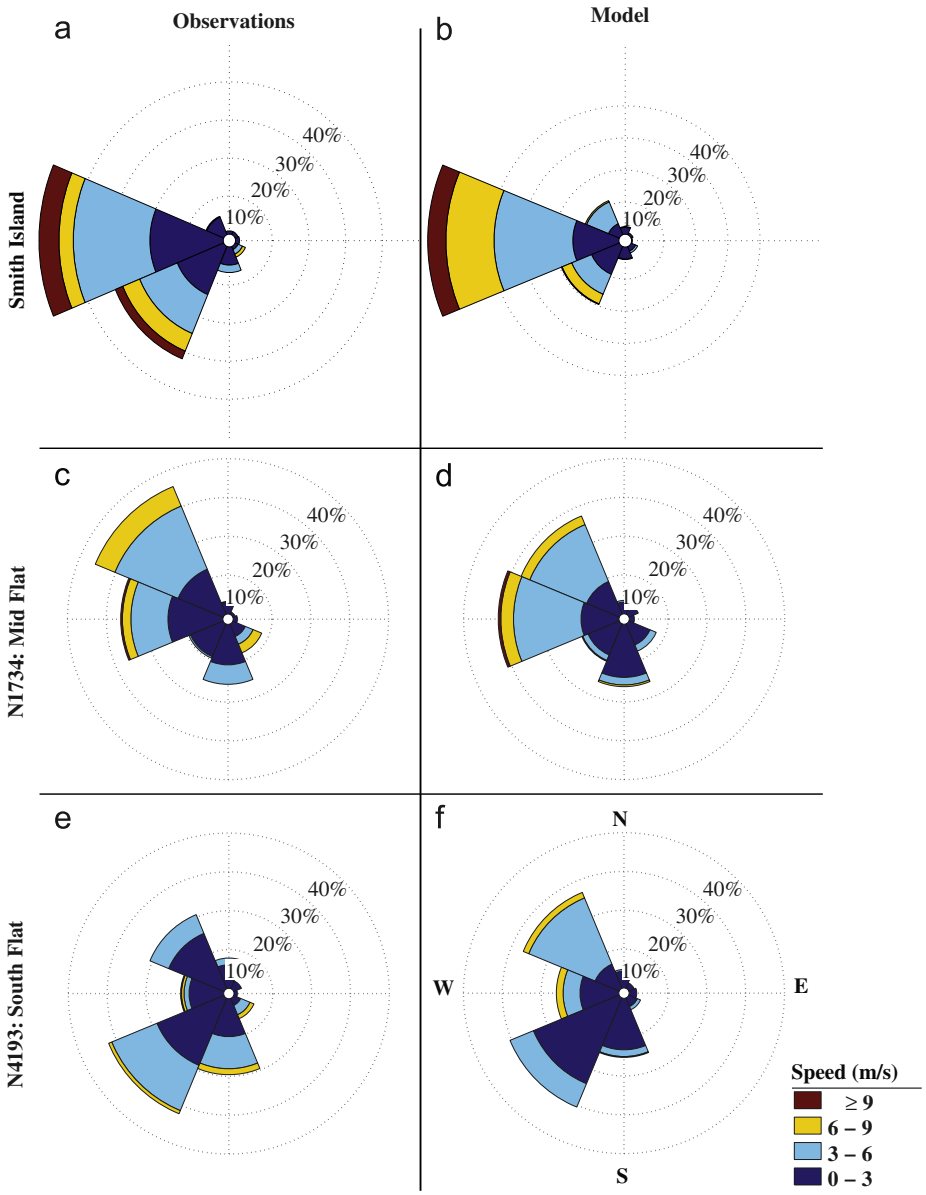

Fig. 6. Wind roses for (a, c, and e) observed and (b, d, and f) modeled winds at (a and b) Smith Island, on (c and d) the mid flats (at N1734) and on (e and f) the south flats (at N4193). Results for N0 and N1588 are similar to those for N1734, and results for N4941 are similar to those for N4193.

to results for diurnal winds in the central US (Zhang and Zheng, 2004) and Italy (Bianco et al., 2006), the model tends to predict lower-than-observed wind speeds before the morning low, and to predict higher-than-observed wind speeds in the afternoon and evening (Fig. 4a). In addition, the predicted morning change from westerly to southerly winds then back to westerly winds typically leads the observed direction changes by 2 to 3 h (Fig. 4b).

Squared correlation coefficients for wind speeds (Fig. 5a) and directions [Fig. 5b, obtained by splitting the azimuthal values into their respective sine and cosine components, and calculating the canonical correlation coefficient for the resulting four variables (Mardia and Jupp, 2000; Jones, 2006)] measured at different locations decrease approximately exponentially with increasing separation distance. Although the model predicts a larger e-folding decorrelation distance than is observed, the winds are predicted to become decorrelated over distances smaller than the scale of the tidal flats (about 10 km), consistent with the observations. Wind roses show that the predominant observed wind direction on the north and mid flats is W to NW (Fig. 6c), whereas the predominant wind direction on the south flats is SW (Fig. 6e). Winds observed near the west coast of Whidbey Island (at Smith Island NDBC SISW1, Fig. 6a) are predominantly westerly and southwesterly, suggesting that the NW winds on the flats are at least partly owing to the local topography steering large-scale flow. The observed spatial variations in wind statistics (e.g., dominant directions) are predicted reasonably well (compare Fig. 6b, d, and f with Fig. 6a, c, and e).

5. Discussion: spatial variability of the wind field

The good agreement between observed and modeled wind patterns suggests that the WRF model can be used to investigate aspects of the wind field. Here, the spatial heterogeneity and the seasonal variations of the winds are investigated using model simulations. The importance of the spatial variability to modeling coastal circulation also is discussed.

Please cite this article as: Raubenheimer, B., et al., Observations and predictions of summertime winds on the Skagit tidal flats, Washington. Continental Shelf Research (2012), doi:10.1016/j.csr.2012.02.001

5.1. Spatial variations of summer winds

Subtle differences in wind orientation from NW to SW affect the interaction of the flow with the topography, and result in different wind patterns over the bay. When modeled summertime winds are from the NW at N1734 (Fig. 7a), winds at all sensor locations are similar in direction and strength (e.g., Fig. 7c). However, when winds at N4193 are from the SW (Fig. 7d), winds on the north flats are from the SW only about 25% of the time, and instead often come from the W (~30%) or S (~20%), and sometimes from the NW or SE (each about 10% of the time) (Fig. 7b). Model simulations suggest that the variability in winds on the tidal flats for SW winds is owing to funneling through Saratoga Passage and a separation region behind the southern tip of Whidbey Island (Fig. 8, winds are SW at N4193 and SE at N1734). The location of the separation zone is sensitive to the large-scale wind magnitude and direction, and small shifts in position result in changes in the winds measured at N1734. The formation of the separation zone behind the hills on Whidbey Island is consistent with low Froude number flows that pass around three-dimensional features (Drazin, 1961; Smith, 1979; Baines, 1979). Thus, steering of westerly winds by the topography of Whidbey Island appears to be important for generating spatial heterogeneity in the winds over Skagit Bay.

5.2. Simulated seasonal variations

During the summer, diurnal fluctuations associated with solar heating dominate the wind variability in this region. However, wind fluctuations with 2–5 d periods (e.g., storms) become increasingly important along the Pacific Northwest coast in the late fall and winter (Tinis et al., 2006). Thus, it is expected that decorrelation distances and spatial wind variations also will vary seasonally. On the Skagit tidal flats, the decorrelation distances for modeled wind speeds and directions increase significantly from summer (July-August) through the fall (September-October)

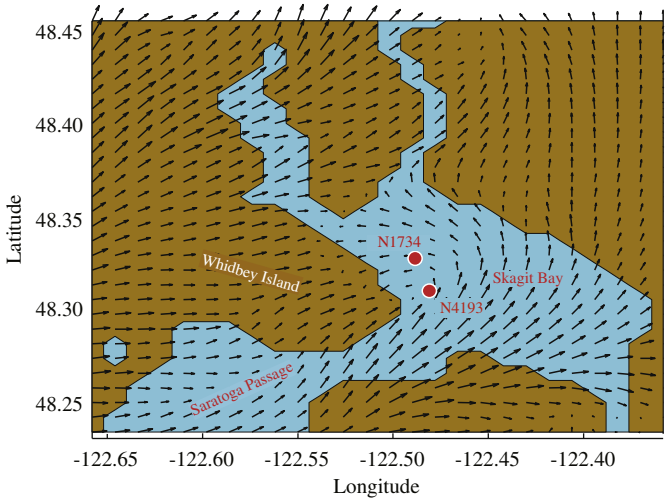

Fig. 8. Modeled 1-h-averaged wind speeds and directions (length and orientation of vectors) for a case with large-scale winds from the west-southwest. Brown is land and blue is water. Locations of N1734 and N4193 are shown by the red circles. Maximum wind speeds for this case are about 8 m s^{-1}. Winds from the WSW and SW funnel through Saratoga Passage, creating a separation zone behind Whidbey Island.

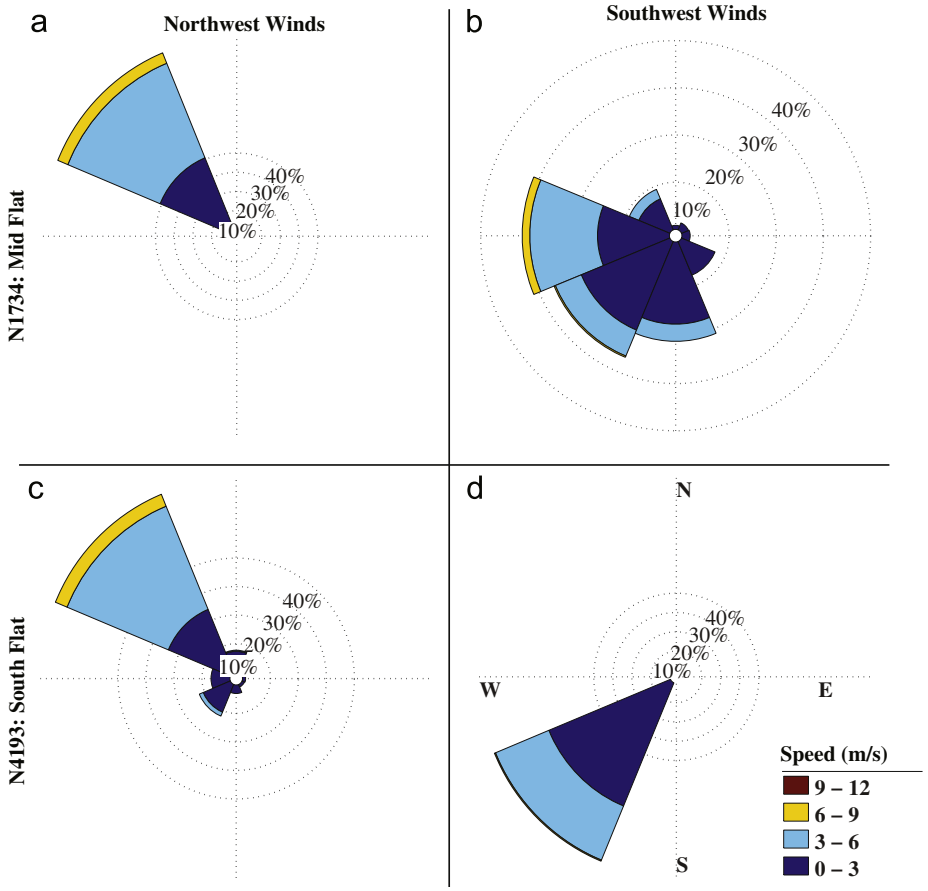

Fig. 7. Wind roses for modeled winds at (a and b) N1734 and (c and d) N4193 when (a and c) winds at N1734 are from the northwest and when (b and d) the winds at N4193 are from the southwest.

Please cite this article as: Raubenheimer, B., et al., Observations and predictions of summertime winds on the Skagit tidal flats, Washington. Continental Shelf Research (2012), doi:10.1016/j.csr.2012.02.001

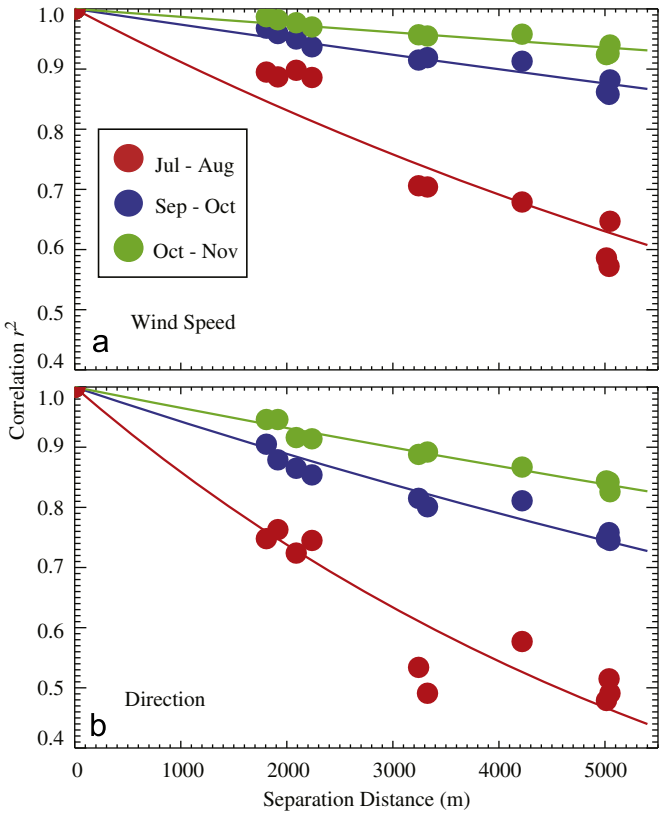

Fig. 9. Squared correlations for modeled (a) wind speed and (b) wind direction at all pairs of anemometers on the tidal flats during July-August (red circles), September-October (blue circles), and November-December, 2009 (green circles) versus separation distance between each pair of locations. The best-fit exponential decays are shown by the colored curves.

to early winter (November-December) (Fig. 9), presumably associated with the larger spatial scales associated with strong frontal systems. Winds in the late winter (January-February) and in the spring (March-May) are similar to those in the early winter and the fall, respectively (not shown). In the fall (and spring), strong winds from the south and southeast with speeds $>9\ \mathrm{m\ s^{-1}}$ are more common than during July (compare Fig. 10a with Fig. 6b and Fig. 10c with Fig. 6d). Spatial gradients in wind direction during the fall (and spring) are similar to those in July, with westerly winds occurring less frequently and southwesterly winds occurring more frequently at N4193 than at N1734. These spatial differences are associated with interactions between the diurnal winds and the local topography. In the early (and late) winter, winds are stronger and predominantly southerly and southeasterly at both N4193 and N1734. Thus, the model predicts that during the passage of fall and winter storms, winds are from the S and SE with speeds reaching $20\ \mathrm{m\ s^{-1}}$ and that the wind speeds and directions during these storms are highly correlated across the tidal flats. Winds measured at Smith Island and at Mt. Vernon in 2009 are representative of those measured at the same location over the past 10 years, suggesting that the model results for 2009 are relevant to typical storm conditions. Thus, these results suggest that winds during storms might be represented well by measurements at a single location on the flats.

5.3. *Modeling coastal circulation*

When modeling coastal circulation, winds often are assumed to be spatially uniform, and wind data from the nearest publically available source commonly are used. Despite the few-km decorrelation length scales (Fig. 5), the predictive skill of three-dimensional hydrodynamic model simulations for salinity and stratification on the south flats (near stations N4193 and N4941) forced with spatially uniform winds based on local wind

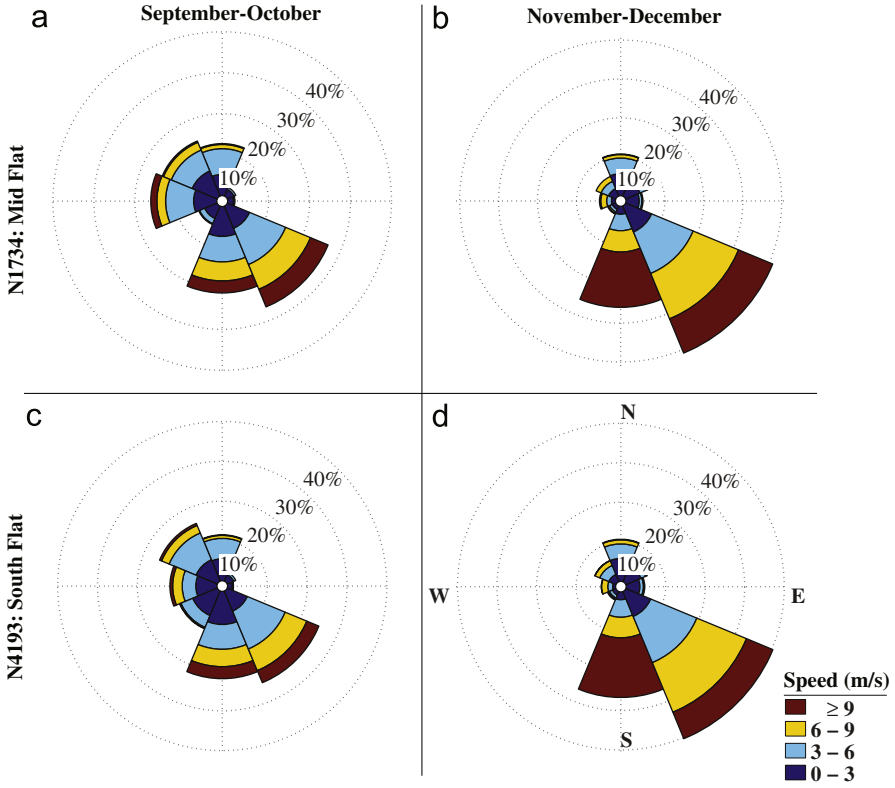

Fig. 10. Wind roses for modeled winds at (a and b) N1734 and (c and d) N4193 during (a and c) September and October and (b and d) November and December, 2009.

Please cite this article as: Raubenheimer, B., et al., Observations and predictions of summertime winds on the Skagit tidal flats, Washington. Continental Shelf Research (2012), doi:10.1016/j.csr.2012.02.001

measurements (from station N4193) is similar to the skill when the model is forced by WRF-simulated, spatially heterogeneous winds (Ralston et al., this issue). For example, the average model skill score (Murphy, 1988) for salinity at 7 observation stations on the south flats is 0.51 using wind forcing from station N4193 and 0.40 for WRF-simulated winds. The corresponding correlation coefficients (r^2) are 0.68 and 0.64. Predictions of surface salinity are sensitive to the local wind direction, which affects the frontal location of the river plume. The good predictive skill using local wind measurements suggests that the local hydrodynamic conditions are not sensitive to the wind forcing a few km away, where the winds may be different. However, the salinity and stratification predictions are less accurate (average skill score is 0.10 and r^2 is 0.49) when the hydrodynamic model is forced with spatially uniform winds from Smith Island (NDBC SISW1), the nearest coastal wind station. Based on these model results, and the decorrelation distances for the winds (Fig. 5), it is expected that accurate modeling of the summertime salinity and stratification requires forcing with either local (within a few km) winds or WRF simulated winds.

Although there are several land-based weather stations that are closer to the flats than Smith Island, the winds are affected by local topography, and the statistical wind magnitudes and directions differ significantly from those on the flats. For example, 4 km east of N1588 at the Washington State University AgWeatherNet Fir Island station (http://weather.wsu.edu/; and 48.36°N, 122.42°W), wind speeds during July and August, 2009 are biased low, with few measurements greater than 3 m s^{-1}, with occasional winds from the northeast and east, but infrequent winds from the west or northwest. Wind speeds measured on the flats are correlated better with those measured at Smith Island than with those measured at Fir Island. Thus, use of land-based wind data, rather than Smith Island wind data, is not expected to improve hydrodynamic model performance on the Skagit tidal flats.

6. Conclusions

Comparisons of wind speeds and directions measured in summer 2009 on the Skagit tidal flats with predictions of the Weather Research and Forecast model suggest that the statistics of wind speeds and directions are predicted reasonably well. In particular, the model predicts the diurnal fluctuations of the winds, with maximum wind speeds occurring in late afternoon and minimum wind speeds occurring in early morning. Additionally, the model predicts that summertime wind speeds and directions are decorrelated over distances shorter than the scale of the flats (about 10 km), consistent with the observations. Observed and predicted wind directions are predominantly W and NW on the north flats, and SW and S on the south flats. Simulations suggest that the variability of the wind directions may result from funneling of winds around the hills on Whidbey Island and through Saratoga Passage. Simulations also suggest that decorrelation distances increase significantly during fall and early winter, as the diurnal winds weaken and passage of strong (larger-scale) frontal systems becomes more common. The observed and predicted spatial heterogeneity of the summertime winds imply that incorporating high-resolution wind models may improve the skill of simulations of coastal circulation on the tidal flats.

Acknowledgments

We thank Jim Thomson for providing the wind measurements collected on Craft Island, the Skagit River System Cooperative and Greg Hood for logistical assistance during the field study, Chuck Long for advice on converting observed winds to 10-m winds, and W. Boyd, S. Burnet, D. Darnell, L. Gorrell, S. Kilgallin, E. Ladouceur, V. Pavel, L. Siegel, E. Williams, R. Yopak, and S. Zippel for helping obtain the field observations. The Office of Naval Research, the National Science Foundation, and a National Security Science and Engineering Faculty Fellowship provided support.

References

Baines, P.G., 1979. Observations of stratified flow past three-dimensional barriers. Journal of Geophysical Research 84, 7834–7838.
Bianco, L., Tomassetti, B., Coppola, E., Fracassi, A., Verdecchia, M., Visconti, G., 2006. Thermally driven circulation in a region of complex topography: comparison of wind-profiling radar measurements and MM5 numerical predictions. Annales de Geophysicae 24, 1537–1549.
Boldt, K.V., Nittrouer, C.A., Ogston, A.S., Seasonal transfer and net accumulation of fine sediment on a muddy tidal flat: Willapa Bay, Washington. Continental Shelf Research, submitted for publication.
Burchard, H., 2009. Combined effects of wind, tide, and horizontal density gradients on stratification in estuaries and coastal seas. Journal of Physical Oceanography 39, 2117–2135.
Carniello, L., Defina, A., Fagherazzi, S., D'Alpaos, L., 2005. A combined wind wave-tidal model for the Venice lagoon, Italy. Journal of Geophysical Research, 110. doi:10.1029/2004JF000232.
Charnock, H., 1955. Wind stress over a water surface. Quarterly Journal of the Royal Meteorological Society 81, 639–640.
Chen, F., Dudhia, J., 2001. Coupling an advanced landsurface/hydrology model with the Penn State/NCAR MM5 modeling system. Monthly Weather Review 129, 569–585.
Cheng, W.Y.Y., Steenburgh, W.J., 2005. Evaluation of Surface Sensible Weather Forecasts by the WRF and the Eta Models over the Western United States. Weather Forecasting 20, 812–821.
Christiansen, C., Vølund, G., Lund-Hansen, L., Bartholdy, J., 2006. Wind influence on tidal flat sediment dynamics: Field investigations in the Ho Bugt, Danish Wadden Sea. Marine Geology 235, 75–86.
Christie, M., Dyer, K., Turner, P., 1999. Sediment flux and bed level measurements from a macrotidal mudflat. Estuarine, Coastal and Shelf Science 49, 667–688.
Chien, F.-C., Mass, C.F., 1997. Interaction of a Warm-Season Frontal System with the Coastal Mountains of the Western United States. Part II: Evolution of a Puget Sound Convergence Zone. Monthly Weather Review 125, 1730–1752.
Cowles, G.W., Lentz, S.J., Chen, C., Xu, Q., Beardsley, R.C., 2008. Comparison of observed and model-computed low frequency circulation and hydrography on the New England Shelf. Journal of Geophysical Research, 113. doi:10.1029/2007JC004394.
Davis, Christopher, et al., 2008. Prediction of Landfalling Hurricanes with the Advanced Hurricane WRF Model. Monthly Weather Review 136, 1990–2005.
Drazin, P.G., 1961. On the steady flow of fluid of variable density past an obstacle. Tellus 13, 239–251.
Dyer, K., Christie, M., Wright, E., 2000. The classification of intertidal mudflats. Continental Shelf Research 20, 1039–1060.
Fagherazzi, S., Palermo, C., Rulli, M., Carniello, L., Defina, A., 2007. Wind waves in shallow microtidal basins and the dynamic equilibrium of tidal flats. Journal of Geophysical Research, 112. doi:10.1029/2006JF000572.
Ferber, G.K., Mass, C.F., 1990. Surface pressure perturbations produced by an isolated mesoscale topographic barrier. Part II: Influence on regional circulation. Monthly Weather Review 118, 2597–2606.
Foreman, M.G.G., Callendar, W., MacFadyen, A., Hickey, B.M., Thomson, R.E., Di Lorenzo, E., 2008. Modeling the generation of the Juan de Fuca Eddy. Journal of Geophysical Research, 113. doi:10.1029/2006JC004082.
Friedrichs, C., Aubrey, D., 1996. Uniform bottom shear stress and equilibrium hypsometry of intertidal flats. In: Pattiaratchi, C., Wash., A.G.U. (Eds.), Mixing in Estuaries and Coastal Seas, 50. Coastal and Estuarine Studies, D.C.
Geyer, W., Trowbridge, J., Bowen, M., 2000. The dynamics of a partially mixed estuary. Journal of Physical Oceanography 30, 2035–2048.
Hanna, S.R., Yang, R., 2001. Evaluations of mesoscale models' simulations of near-surface winds, temperature gradients, and mixing depths. Journal of Applied Meteorology 40, 1095–1104.
Henderson, S.M., Mullarney, J.C., Wave mixed, wind generated near-surface shear observed over a tidal flat. Continental Shelf Research, submitted for publication.
Jones, T.A., 2006. MATLAB functions to analyze directional (azimuthal) data–II: Correlation. Computers and Geosciences 32, 176–183. doi:10.1016/j.cageo.2005.06.021.
Kraus, E., 1972. Atmosphere-Ocean interaction. Oxford University Press, London, 275 pp.
Le Hir, P., Roberts, W., Cazaillet, O., Christie, M., Bassoullet, P., Bacher, C., 2000. Characterization of intertidal flat hydrodynamics. Continental Shelf Research 20, 1433–1459.
Liu, Y., MacCready, P., Hickey, B.M., 2009. Columbia River plume patterns in summer 2004 as revealed by a hindcast coastal ocean circulation model. Geophysical Research Letters, 36. doi:10.1029/2008GL036447.

Please cite this article as: Raubenheimer, B., et al., Observations and predictions of summertime winds on the Skagit tidal flats, Washington. Continental Shelf Research (2012), doi:10.1016/j.csr.2012.02.001

Manning, A., Bass, S., 2006. Variability in cohesive sediment settling fluxes: Observations under different estuarine tidal conditions. Marine Geology 235, 177–192.

Manning, A., Bass, S., Dyer, K., 2006. Floc properties in the turbidity maximum of a mesotidal estuary during neap and spring tidal conditions. Marine Geology 235, 193–211.

Mardia, K.V., Jupp, P.E., 2000. Directional Statistics, 2nd edition John Wiley and Sons Ltd., ISBN: 0-471-95333-4 460 pp.

Mariotti, G., Fagherazzi, S., Wind waves on a mudflat: the influence of fetch and depth on bottom shear stresses. Continental Shelf Research, doi:10.1016/j.csr.2012.03.001, this issue.

Mass, C.F., 1981. Topographically forced convergence in western Washington State. Monthly Weather Review 109, 1335–1347.

Miao, J.-F., Wyser, K., Chen, D., Ritchie, H., 2009. Impacts of boundary layer turbulence and land surface process parameterizations on simulated sea breeze characteristics. Annales de Geophysicae 27, 2303–2320.

Moeng, C.-H., Dudhia, J., Klemp, J., Sullivan, P., 2007. Examining two-way grid nesting for large eddy simulation of the PBL using the WRF model. Monthly Weather Review 135, 2295–2311.

Murphy, A.H., 1988. Skill scores based on the mean square error and their relationships to the correlation coefficient. Monthly Weather Review 116, 2417–2424.

Nowacki, D.J., Ogston, A.S., Water and sediment transport of channel-flat systems in a mesotidal mudflat: Willapa Bay, Washington. Continental Shelf Research, submitted for publication.

Orlíc, M., Penzar, B., Penzar, I., 1988. Adriatic sea and land breezes: Clockwise versus anticlockwise rotation. Journal of Applied Meteorology 27, 675–679.

Peña, A., Gryning, S.-E., 2008. Charnock's Roughness Length Model and Non-dimensional Wind Profiles Over the Sea. Boundary-Layer Meteorology 128, 191–203.

Prtenjak, M.T., Grisogono, B., 2007. Sea/land breeze climatological characteristics along the northern Croatian Adriatic coast. Theoretical and Applied Climatology 90, 201–215.

Ralston, D.K., Stacey, M., 2007. Tidal and meteorological forcing of sediment transport in tributary mudflat channels. Continental Shelf Research 27, 1510–1527.

Ralston, D.K., Geyer, W.R., Traykovski, P.A., Nidzieko, N.J., Effects of estuarine and fluvial processes on sediment transport over deltaic tidal flats. Continental Shelf Research, doi:10.1016/j.csr.2012.02.004, this issue.

Rosero, E., Yang, Z.-L., Gulden, L.E., Niu, G.-Y., Gochis, D.J., 2009. Evaluating Enhanced Hydrological Representations in Noah LSM over Transition Zones: Implications for Model Development. Journal of Hydrometeorology 10, 600–622.

Scully, M., Friedrichs, C., Brubaker, J., 2005. Control of estuarine stratification and mixing by wind-induced straining of the estuarine density field. Estuaries 28, 321–326.

Sempreviva, A., Larsen, S., Mortensen, N., Troen, I., 1990. Response of neutral boundary layers to changes of roughness. Boundary-Layer Meteorology 50, 205–225.

Simpson, J.E., 1996. Diurnal changes in sea-breeze direction. Journal of Applied Meteorology 35, 1166–1169.

Skamarock, W.C., Klemp, J.B., Dudhia, J., Gill, D.O., Barker, D.M., Duda, M.G., Huang, X.-Y., Wang, W., Powers, J.G., 2008. A description of the Advanced Research WRF, version 3. NCAR Tech. Note NCAR/TN-475+STR, 125 pp. [Available from UCAR Communications, P.O. Box 3000, Boulder, CO 80307].

Skogseth, R., Sandvik, A.D., Asplin, L., 2007. Wind and tidal forcing on the mesoscale circulation in Storfjorden, Svalbard. Continental Shelf Research 27, 208–227. doi:10.1016/j.csr.2006.10.001.

Smith, R.B., 1979. The influence of mountains on the atmosphere. Advances in Geophysics, 21. Academic Press 187–230.

Smith, S., 1980. Wind stress and heat flux over the ocean in the gale force winds. Journal of Physical Oceanography 10, 709–726.

Snow, J.A., Dennison, J.B., Jaffe, D.A., Price, H.U., Vaughan, J.K., Lamb, B., 2003. Aircraft and surface observations of air quality in Puget Sound and a comparison to a regional model. Atmospheric Environment 37, 4019–4032. doi:10.1016/S1352-2310(03)00429-1.

Talke, S., Stacey, M., 2008. Suspended sediment fluxes at an intertidal flat: The shifting influence of wave, wind, tidal, and freshwater forcing. Continental Shelf Research 28, 710–725.

Tinis, S., Thomson, R.E., Mass, C., Hickey, B.M., 2006. Comparison of MM5 and meteorological buoy winds from British Columbia to northern California. Atmosphere—Ocean 44, 65–81.

Valle-Levinson, A., Reyes, C., Sanay, R., 2003. Effects of bathymetry, friction, and rotation on estuary-ocean exchange. Journal of Physical Oceanography 33, 2375–2393.

Webster, K.L., Ogston, A.S., Nittrouer, C.A. Delivery, reworking, and export of fine-grained sediment across the sandy Skagit River tidal flats. Continental Shelf Research, submitted for publication.

Yang, S., Friedrichs, C., Zhong, S., Ping-Xing, D., Zhu, J., Zhao, Q., 2003. Morphological response of tidal marshes, flats, and channels of the Outer Yangtze River mouth to a major storm. Estuaries 26, 1416–1425.

Yang, Z., Khangaonkar, T., Calvi, M., Nelson, K., 2010. Simulation of cumulative effects of nearshore restoration projects on estuarine hydrodynamics. Ecological Modeling 221, 969–977.

Zhang, D.L., Zheng, W.Z., 2004. Diurnal cycles of surface winds and temperature as simulated by five boundary layer parameterizations. Journal of Applied Meteorology 43, 157–169.

Zhong, S.Y., Fast, J., 2003. An evaluation of the MM5, RAMS, and Meso-Eta models at subkilometer resolution using VTMX field campaign data in the Salt Lake valley. Monthly Weather Review 131, 1301–1322.

Zhong, S.Y., Takle, E.S., 1993. The effects of large-scale winds on the sea-land-breeze circulations in an area of complex coastal heating. Journal of Applied Meteorology 32, 1181–1195.

Please cite this article as: Raubenheimer, B., et al., Observations and predictions of summertime winds on the Skagit tidal flats, Washington. Continental Shelf Research (2012), doi:10.1016/j.csr.2012.02.001